Bounds on dissipation in magnetohydrodynamic Couette and Hartmann shear flows

A. Alexakis[a)]
Department of Physics, University of Chicago, Chicago, Illinois 60637

F. Pétrélis
Laboratoire de Physique Statistique, ENS, 24 rue Lhomond, 75005 Paris, France

P. J. Morrison[b)]
Department of Physics and Institute for Fusion Studies, The University of Texas at Austin, Austin, Texas 78712

Charles R. Doering
*Department of Mathematics, University of Michigan, Ann Arbor, Michigan 48109-1109
and Michigan Center for Theoretical Physics, Ann Arbor, Michigan 48109-1120*

Shear flow with an applied cross-stream magnetic field is studied using dissipative incompressible magnetohydrodynamics. The study incorporates exact solutions, the energy stability method, and exact bounds on the total energy dissipation rate. Two physical configurations are examined: magnetic Couette flow and Hartmann flow, the latter being Poiseuille flow with the existence of a perpendicular magnetic field. Explicit expressions are derived for energy stability regions in the parameter space and these expressions are compared with numerically obtained results. For large enough Reynolds numbers the energy dissipation rate is shown to be bounded by a function of the magnetic Prandtl number. The bounds obtained on the dissipation rate are compared with experimental results. © *2003 American Institute of Physics.* [DOI: 10.1063/1.1613962]

I. INTRODUCTION

Sheared flow of conducting fluids across magnetic field lines appears in many physical situations ranging from astrophysical to industrial. For instance, accretion in strongly magnetized compact stars is assumed to take place in the polar caps, where the magnetic field is vertical with respect to the surface of the star and the accreted material spreads along the surface perpendicular to the field lines. A similar situation appears when the solar wind meets a magnetized object and the flow has to do work in bending the magnetic field lines emanating from the object. In industry, cross-stream magnetic fields are used in production-line crystal growth to stabilize flow and to control the dopant distribution of the final product. In metallurgy such fields are used as a dumping mechanism, and in fusion plasma devices a liquid metal blanket subject to a strong magnetic field is proposed for reactors. The above mentioned cases have the common feature that a thin layer, known as the Hartmann layer, is formed at the boundary even when the flow is laminar. The stability as well as the properties of the dissipation rate of both the laminar and the turbulent Hartmann layer are important for the subsequent evolution of the astrophysical systems, and the same is true for the control in the industrial applications.

Among the first to examine the effect of a cross-stream magnetic field on shear flow, both theoretically and experi-

mentally, was Hartmann (see Refs. 1 and 2). Hartmann showed that the magnetohydrodynamic (MHD) equations support laminar solutions that exhibit boundary layer structure, and he carried out experiments with flowing liquid metals in rectangular ducts, so-called Hartmann flow. The investigation of Hartmann flow has been further extended experimentally by many researchers (e.g., Refs. 3–6). One of the primary quantities that has been measured is the dependence of the friction coefficient on the magnetic field, which (as shown below) is a function of the total energy dissipation rate. Furthermore, experimental results indicate that the critical Reynolds number, above which the flow becomes turbulent, is in the range $150 < \mathrm{Re}/\mathrm{Ha} < 250$, where Re and Ha are the Reynolds and Hartmann numbers, respectively [see Eqs. (4) and (6) below]. The ratio Re/Ha can be interpreted as an effective Reynolds number inside the Hartmann layer Ref. 7. This is because the thickness of a Hartmann layer scales as d/Ha, which when used as the length scale in the Reynolds number gives $Ud/\mathrm{Ha}/\nu = \mathrm{Re}/\mathrm{Ha}$.

The linear stability of both Hartmann flow, which is sometimes called magnetic Poiseuille flow, and magnetic Couette flow, has been investigated in Refs. 8–10. In Refs. 9 and 10 the critical Reynolds number for linear instability was found to be $\mathrm{Re}/\mathrm{Ha} = 48\,311$, which is much higher than what is observed experimentally. This led Lingwood and Alboussiere in Ref. 11 to examine the so-called energy stability of the Hartmann layer. They found that the Hartmann layer for small Prandtl numbers is energy stable when $\mathrm{Re}/\mathrm{Ha} < 26$.

Due to the fact that both the Couette and Hartmann laminar (equilibrium) solutions are not trivial, both the linear

---

[a)]Electronic mail: alexakis@mhd11.uchicago.edu
[b)]Electronic mail: morrison@physics.utexas.edu

stability and the energy stability equations must be solved numerically. This restricts the range in the parameter space that can be examined, especially since these flows have three independent nondimensional numbers. Furthermore, the analysis of Ref. 11 is restricted to small Prandtl numbers by using an approximation of the MHD equations that is applicable to liquid metals ($P_m \sim 10^{-6}$) and moderate magnetic fields, but not to plasmas ($P_m \sim 10^{-6}-10^{+6}$) or strong magnetic fields. In the present paper we give estimates of the energy stability boundaries of the two types of Hartmann and magnetic Couette flows examined in Refs. 9 and 10, and we compare with numerical results.

Furthermore we derive bounds on the energy dissipation rate of the two aforementioned flows, when the flow is in the turbulent regime. The procedure for bounding such quantities has been developed considerably in recent years. Two main approaches exist, both of which incorporate a splitting of the velocity and magnetic fields into two components, a background field and a perturbation field. The main difference of the approaches lies in the extremizing procedures. The first approach uses a mean field in the manner of Reynolds decomposition, and was first formulated and carried out successfully by Howard in Refs. 12 and 13 and applied widely and effectively by Busse (see, for example, Ref. 14). In plasma physics in the context of MHD it was used in Refs. 15–17. In the second approach, the one we adopt here, the background field plays a more central role in the variational procedures. This method, which is called the *background method*, was developed by Doering and Constantin in Refs. 18 and 19. The background method has close ties to energy stability theory and it too has been applied to a number of fluid problems. Here and in a companion paper (Ref. 20) the background method is used for the first time in plasma physics. The companion paper can be consulted for further discussion of the background method and additional references. We note, Kerswell in Ref. 21 has elucidated a formal mathematical connection between these two approaches for the case of driven shear flows.

The present paper is structured as follows. In Sec. II we describe the problems to be studied, define the quantities we are going to estimate, and present the laminar solutions. In Sec. III we derive estimates for the energy stability boundaries. In Sec. IV we derive bounds for the energy dissipation rate of the flows. A comparison of our results with experimental data is made in Sec. V, where we summarize and conclude.

II. FORMULATION

A. Preliminaries

To investigate the influence of a cross-stream magnetic field on shear flows, we consider a layer of an incompressible conducting fluid of density $\rho \equiv 1$, constant kinematic viscosity ν, and constant magnetic diffusivity (resistivity) η, confined between parallel rigid plates of size L_x, L_z located at $y = -d$ and $y = d$. The velocity field is designated by $\mathbf{v}(x,y,z) = \mathbf{i}v_x + \mathbf{j}v_y + \mathbf{k}v_z$, and the magnetic field by
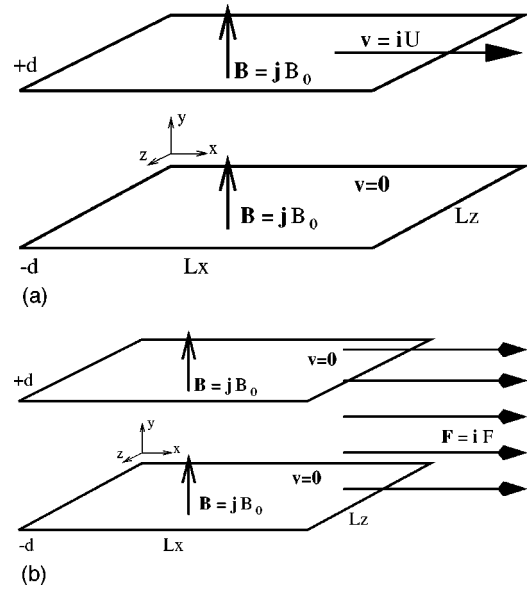

FIG. 1. Panel (a) shows the setup for magnetic Couette flow and panel (b) shows the setup for Hartmann flow.

$\mathbf{B}(x,y,z) = \mathbf{i}B_x + \mathbf{j}B_y + \mathbf{k}B_z$, where both $\mathbf{v}$ and $\mathbf{B}$ are measured in units of velocity. The system is assumed to be governed by MHD equations,

$$\frac{\partial \mathbf{v}}{\partial t} + \mathbf{v} \cdot \nabla \mathbf{v} = -\nabla P + \mathbf{B} \cdot \nabla \mathbf{B} + \nu \nabla^2 \mathbf{v} + \mathbf{F}, \tag{1}$$

where $P := p + B^2/2$, with p being the hydrodynamic pressure, and $\mathbf{F}$ is an applied force,

$$\frac{\partial \mathbf{B}}{\partial t} + \mathbf{v} \cdot \nabla \mathbf{B} = \mathbf{B} \cdot \nabla \mathbf{v} + \eta \nabla^2 \mathbf{B}, \tag{2}$$

and the divergence-free constraints,

$$\nabla \cdot \mathbf{v} = 0, \quad \nabla \cdot \mathbf{B} = 0. \tag{3}$$

We assume periodic boundary conditions in the x and z directions for all fields. For the y direction we use no slip for the velocity field $\mathbf{v}(x,-d,z) = 0$ and $\mathbf{v}(x,d,z) = \mathbf{i}U$, where U is the velocity of the top plate. For the magnetic field we use the "line-tied" boundary conditions, $\mathbf{B}(x,\pm d,z) = \mathbf{j}B_0$, where B_0 is the imposed cross-stream magnetic field. (See Ref. 20 for a discussion of the physical relevance of these and other boundary conditions used for MHD.)

We consider two problems with the configurations depicted in Fig. 1. For the first one, magnetic Couette flow, we set $\mathbf{F} = 0$ and $U \neq 0$. The setup for this problem is shown in Fig. 1(a). We nondimensionalize lengths by d (so $y \in [-1,1]$) and velocities by U. Three independent nondimensional numbers emerge from this scaling: the Reynolds number

$$\text{Re} := \frac{Ud}{\nu}, \tag{4}$$

the magnetic Reynolds number

$$R_m := \frac{Ud}{\eta}, \tag{5}$$

and the Hartmann number given by

$$\text{Ha} := \frac{B_0 d}{\sqrt{\nu \eta}}. \tag{6}$$

We note that instead of the magnetic Reynolds number we could equivalently use the magnetic Prandtl number $P_m = \nu / \eta$; the two are related by $R_m = \text{Re}\, P_m$.

For the second problem, that of Hartmann flow, $U = 0$ and $\mathbf{F} = \mathbf{i}F$. This setup is shown in Fig. 1(b). For this problem again we use the length scale d, but the velocities are now scaled by $\sqrt{Fd}$. The nondimensional numbers that result are the Grashoff number,

$$\text{Gr} := \frac{Fd^3}{\nu^2}, \tag{7}$$

the magnetic Grashoff number,

$$G_m := \frac{Fd^3}{\nu \eta}, \tag{8}$$

and the Hartmann number given by Eq. (6). The magnetic Grashoff number and the magnetic Prandtl are related by $G_m = \text{Gr}\, P_m$.

The time and space averaged total rate of energy dissipation, viscous plus Ohmic, for both problems is defined to be

$$\bar{\mathcal{D}} := \nu \overline{\langle |\nabla \mathbf{v}|^2 \rangle} + \eta \overline{\langle |\nabla \mathbf{B}|^2 \rangle}, \tag{9}$$

where we introduce our notation for space averages,

$$\langle f \rangle = \frac{1}{2\, dL_x L_z} \int_0^{L_x} dx \int_0^{L_z} dz \int_{-d}^{+d} dy\, f \tag{10}$$

and time space averages,

$$\overline{\langle f \rangle} = \lim_{T \to \infty} \frac{1}{T} \int_0^T \langle f \rangle dt. \tag{11}$$

A nondimensional form of the dissipation rate can be defined as

$$\bar{\mathcal{D}} = \frac{U^3}{d} \phi \tag{12}$$

for Couette flow and

$$\bar{\mathcal{D}} = F^{3/2} d^{1/2} \psi \tag{13}$$

for Hartmann flow, where obtaining information about the functions ϕ and ψ is one of our main goals.

Many works use the Reynolds number prescribed by the mean flow $\text{Re} := \overline{\langle v_x \rangle} d / \nu$ instead of the Grashoff number. A relationship between the Grashoff number and the Reynolds number can be obtained by taking the scalar product of Eq. (1) with $\mathbf{v}$ and Eq. (2) with $\mathbf{B}$, time and space averaging, and then adding them together. This gives the energy conservation equation $F\overline{\langle v_x \rangle} = \bar{\mathcal{D}}$, where it is assumed that the energy of the flow remains bounded in time and consequently the time derivative term drops out upon time averaging. The energy conservation equation can be rearranged to give

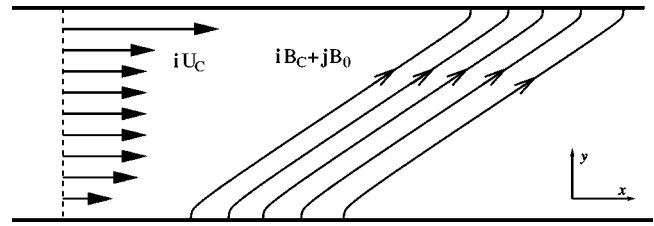$$\text{Re} = \psi\, \text{Gr}^{1/2}. \tag{14}$$

FIG. 2. Velocity profile and the magnetic field lines for magnetic Couette flow.

If we define the energy dissipation rate for the Hartmann flow problem as

$$\bar{\mathcal{D}} = \frac{\overline{\langle v_x \rangle}^3}{d} \phi, \tag{15}$$

we obtain the following relation between the two nondimensional dissipations:

$$\phi = \psi^{-2}. \tag{16}$$

Finally, the friction coefficient C_f that is often measured in experiments can be shown to be equal to ϕ in this scaling,

$$C_f := \frac{Fd}{\overline{\langle v_x \rangle}^2} = \phi. \tag{17}$$

B. Laminar solutions

First we consider magnetic Couette flow. Equations (1) and (2) have a laminar solution given by $\mathbf{v} = \mathbf{i}U_C$ and $\mathbf{B} = \mathbf{i}B_C + \mathbf{j}B_0$ where

$$U_C(y) = \frac{U}{2}\left[1 + \frac{\sinh(\text{Ha}\, y)}{\sinh(\text{Ha})} \right] \tag{18}$$

and

$$B_C(y) = \frac{U}{2} P_m^{1/2}\left[\frac{\cosh(\text{Ha}) - \cosh(\text{Ha}\, y)}{\sinh(\text{Ha})} \right]. \tag{19}$$

This flow reduces to ordinary Couette flow in the limit Ha $\to 0$. The laminar velocity and the magnetic field lines are shown in Fig. 2.

The energy dissipation rate of this laminar flow is given by

$$\mathcal{D}_C = \frac{U^3}{4d} \frac{\text{Ha}}{\text{Re}} \coth(\text{Ha}). \tag{20}$$

Similarly, Hartmann flow has the laminar solution

$$U_H = \sqrt{Fd}\, \frac{\text{Gr}^{1/2}}{\text{Ha}}\left[\frac{\cosh(\text{Ha}) - \cosh(\text{Ha}\, y)}{\sinh(\text{Ha})} \right] \tag{21}$$

and

$$B_H = \sqrt{Fd}\, \frac{G_m^{1/2}}{\text{Ha}}\left[\frac{\sinh(\text{Ha}\, y)}{\sinh(\text{Ha})} - y \right]. \tag{22}$$

The laminar velocity and the magnetic field lines of this flow are shown in Fig. 3. Again the limit Ha $\to 0$ brings us back to ordinary Poiseuille flow. The dissipation rate of this laminar solution is
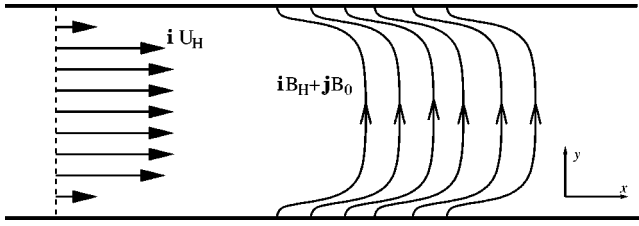
Phys. Plasmas, Vol. 10, No. 11, November 2003

Bounds on dissipation in magnetohydrodynamic Couette . . . 4327

FIG. 3. Velocity profile and the magnetic field lines for Hartmann flow.

$$\bar{\mathcal{D}}_H = \sqrt{F^3 d}\,\frac{\mathrm{Gr}^{1/2}}{\mathrm{Ha}}\left[\coth(\mathrm{Ha}) - \frac{1}{\mathrm{Ha}}\right]. \tag{23}$$

The Reynolds number for the laminar flow can be obtained using Eqs. (14) and (23).

C. Background decomposition

A device that we are going to use throughout this paper is to decompose the velocity and the magnetic fields into steady background components $\mathbf{i}U_b$ and $\mathbf{i}B_b$, which depend only on the y coordinate, and perturbation fields $\mathbf{u}$ and $\mathbf{b}$, which depend on all space coordinates and time as follows:

$$\mathbf{v} = \mathbf{i}U_b(y) + \mathbf{u}, \tag{24}$$

$$\mathbf{B} = \mathbf{i}B_b(y) + \mathbf{j}B_0 + \mathbf{b}, \tag{25}$$

where B_0 is constant. The background fields satisfy the same boundary conditions as the fields $\mathbf{v}$ and $\mathbf{B}$, but they need not be equal to the laminar solutions of Sec. II B. The time evolution of the fields $\mathbf{u}$ and $\mathbf{b}$ are given, respectively, by

$$\frac{\partial \mathbf{u}}{\partial t} + \mathbf{u} \cdot \nabla \mathbf{u} + U_b \frac{\partial \mathbf{u}}{\partial x} + \mathbf{i}u_y U_b'$$

$$= \mathbf{b} \cdot \nabla \mathbf{b} + B_b \frac{\partial \mathbf{b}}{\partial x} + \mathbf{i}B_0 B_b' + B_0 \frac{\partial \mathbf{b}}{\partial y}$$

$$+ \mathbf{i}b_y B_b' + \nu(\mathbf{i}U_b'' + \nabla^2 \mathbf{u}) - \nabla P + \mathbf{i}F \tag{26}$$

and

$$\frac{\partial \mathbf{b}}{\partial t} + \mathbf{u} \cdot \nabla \mathbf{b} + U_b \frac{\partial \mathbf{b}}{\partial x} + \mathbf{i}u_y B_b'$$

$$= \mathbf{b} \cdot \nabla \mathbf{u} + B_b \frac{\partial \mathbf{u}}{\partial x} + \mathbf{i}B_0 U_b' + B_0 \frac{\partial \mathbf{u}}{\partial y}$$

$$+ \mathbf{i}b_y U_b' + \eta(\mathbf{i}B_b'' + \nabla^2 \mathbf{b}), \tag{27}$$

where prime denotes differentiation with respect to y. Both $\mathbf{u}$ and $\mathbf{b}$ satisfy the divergence-free constraint and the boundary conditions

$$\mathbf{u}(x, \pm d, z) = 0 \quad \text{and} \quad \mathbf{b}(x, \pm d, z) = 0. \tag{28}$$

Taking the scalar product of Eq. (26) with $\mathbf{u}$ and (27) with $\mathbf{b}$, adding, and then taking the space average we obtain the equation for the evolution of $\mathcal{E} := \langle u^2 + b^2 \rangle/2$, an energy-like quantity for the fluctuating fields,

$$\frac{d\mathcal{E}}{dt} = \langle u_x B_0 B_b' \rangle + \langle b_x B_0 U_b' \rangle + \langle (b_x b_y - u_x u_y) U_b' \rangle$$

$$+ \langle (u_x b_y - u_y b_x) B_b' \rangle - \eta \langle |\nabla \mathbf{b}|^2 \rangle - \nu \langle |\nabla \mathbf{u}|^2 \rangle$$

$$+ \nu \langle u_x U_b'' \rangle + \eta \langle b_x B_b'' \rangle + \langle u_x F \rangle, \tag{29}$$

where many terms have dropped out due to the boundary conditions (28).

III. STABILITY

The stability or instability of a steady laminar flow determines its realizability. The linear stability of the magnetic Couette and Hartmann laminar solutions can be investigated by expanding about them, dropping the nonlinear terms in (26) and (27), assuming a dependence of the form $e^{\gamma t}e^{ik_x x + ik_z z}$ for all fields, and solving the resulting eigenvalue problem for γ. This problem has been investigated for both the magnetic Couette and the Hartmann flows by Takashima in Refs. 9 and 10. He examined a wide region of the parameter space $(\mathrm{Re}, P_m, \mathrm{Ha})$ and found for small magnetic Prandtl numbers $(P_m = 10^{-8})$ that the effective critical Reynolds number is given by $\mathrm{Re}/\mathrm{Ha} \simeq 4.8311 \times 10^4$ for both problems. This number was shown to decrease as the Prandtl number increases. The experimental value for instability is two orders of magnitude smaller than Takashima's result and lies in the range $150 < \mathrm{Re}/\mathrm{Ha} < 250$.

In this section we consider a different kind of stability, so-called energy (or nonlinear) stability. Lingwood and Alboussiere in Ref. 11 first investigated the energy stability of the Hartmann layer with a semi-infinite domain in the limit of small Prandtl number, and found a critical value of the effective Reynolds number of $\mathrm{Re}/\mathrm{Ha} = 26$. This value is one order of magnitude smaller than that obtained by experiment. As Lingwood and Alboussiere note, this value should be interpreted as a lower bound for instability to occur. We obtain energy stability results for both magnetic Couette and Hartmann flows with extended parameter ranges, and for the sake of comparison the linear stability of Hartmann flow has been analyzed.

A. Energy stability

In order to investigate energy stability we suppose that the two background fields in (24) and (25) are either of the magnetic Couette or Hartmann laminar solutions, i.e., we suppose $U_b(y) = U_l(y)$ and $B_b(y) = B_l(y)$, where $l = C$ or H. Thus, Eqs. (26) and (27) reduce to

$$\frac{\partial \mathbf{u}}{\partial t} + \mathbf{u} \cdot \nabla \mathbf{u} + U_l \frac{\partial \mathbf{u}}{\partial x} + \mathbf{i}u_y U_l'$$

$$= -\nabla P + B_l \frac{\partial \mathbf{b}}{\partial x} + B_0 \frac{\partial \mathbf{b}}{\partial y} + \mathbf{i}b_y B_l' + \mathbf{b} \cdot \nabla \mathbf{b} + \nu \nabla^2 \mathbf{u}, \tag{30}$$

$$\frac{\partial \mathbf{b}}{\partial t} + \mathbf{u} \cdot \nabla \mathbf{b} + U_l \frac{\partial \mathbf{b}}{\partial x} + \mathbf{i}u_y B_l'$$

$$= B_l \frac{\partial \mathbf{u}}{\partial x} + B_0 \frac{\partial \mathbf{u}}{\partial y} + \mathbf{i}b_y U_l' + \mathbf{b} \cdot \nabla \mathbf{u} + \eta \nabla^2 \mathbf{b}, \tag{31}$$

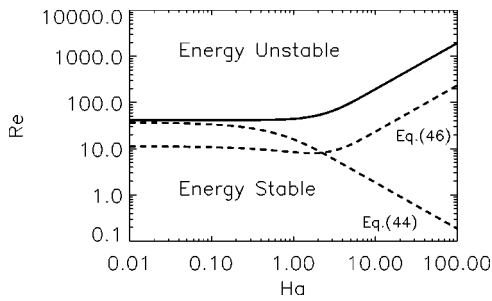and Eq. (29) for $\mathcal{E}$ can be written as

FIG. 4. Critical Reynolds number for Couette flow as a function of Ha for $P_m = 1$. The solid line is the numerical solution of (39) and the dashed lines are the derived bounds of (44) and (46). The bounds of Sec. III B imply that the laminar solution is energy stable for points below either of the dashed curves.
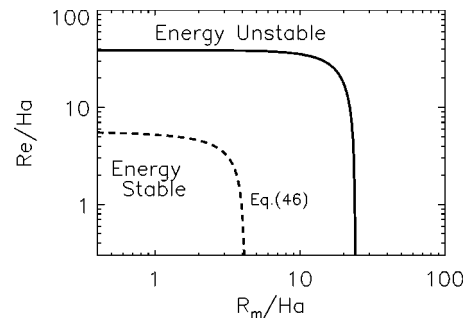

FIG. 5. Stability boundary for large Ha for Couette flow. The solid line is a numerical solution for Ha = 100 and the dashed line is the derived bound of (46).

$$\frac{d\mathcal{E}}{dt} = -\mathcal{F}_l[\mathbf{u},\mathbf{b}], \tag{32}$$

where the functional

$$\mathcal{F}_l[\mathbf{u},\mathbf{b}] := \langle \nu|\nabla\mathbf{u}|^2 + \eta|\nabla\mathbf{b}|^2 + (u_x u_y - b_x b_y)U_l'$$
$$+ (b_x u_y - u_x b_y)B_l' \rangle \tag{33}$$

is a homogeneous quadratic form in $\mathbf{u}$ and $\mathbf{b}$ that depends on the laminar solutions U_l and B_l.

Energy stability rests on the observation that if $\mathcal{F}_l$ is a strongly positive quadratic form, then $\mathcal{E}$ decays exponentially in time. Strong positivity of $\mathcal{F}_l$ means that there is a positive number λ such that

$$\mathcal{F}_l[\mathbf{u},\mathbf{b}] \geq \lambda\mathcal{E} \tag{34}$$

for all divergence-free vector fields $\mathbf{u}$ and $\mathbf{b}$ satisfying the boundary conditions (28). If (34) is fulfilled then $\mathcal{E}$ satisfies the inequality

$$\frac{d\mathcal{E}}{dt} \leq -\lambda\mathcal{E} \tag{35}$$

and according to Gronwall's lemma, this implies that $\mathcal{E}$ decays at least exponentially, i.e.,

$$\mathcal{E}(t) \leq \mathcal{E}(0)e^{-\lambda t}. \tag{36}$$

The largest possible value of λ that satisfies Eq. (34) is given by

$$\lambda(\mathrm{Re},R_m,\mathrm{Ha}) = \inf \frac{\mathcal{F}_l[\mathbf{u},\mathbf{b}]}{\mathcal{E}}, \tag{37}$$

where the infimum is taken over all divergence-free vector fields $\mathbf{u}$ and $\mathbf{b}$ satisfying the boundary conditions (28). Effecting the minimization procedure leads to the following eigenvalue problem for λ:

$$\mathrm{Re}^{-1}\nabla^2\mathbf{u} + (\mathbf{i}u_y + \mathbf{j}u_x)U_l'/2 + (\mathbf{j}b_x - \mathbf{i}b_y)B_l'/2 - \nabla p = \lambda\mathbf{u}, \tag{38}$$

$$R_m^{-1}\nabla^2\mathbf{b} - (\mathbf{i}b_y + \mathbf{j}b_x)U_l'/2 + (\mathbf{i}u_y - \mathbf{j}u_x)B_l'/2 - \nabla q = \lambda\mathbf{b}, \tag{39}$$

where p and q are Lagrange multipliers that impose the divergence-free condition for the two fields. The energy stability boundary in the parameter space is given by those values of Re, R_m, and Ha where $\lambda(\mathrm{Re},R_m,\mathrm{Ha}) = 0$.

We numerically solve for the stability boundary. Fourier expanding in x and z and setting λ and k_x to zero give an eigenvalue problem for $\mathrm{Re}(R_m,\mathrm{Ha})$. The reason we set $k_x = 0$ is because it can be shown that down stream rolls ($k_x = 0$) are local minima. It is believed, and assumed here, that the global minima of interest also have $k_x = 0$. We solve the resulting eigenvalue problem using a Chebyshev collocation technique. The results are shown in Figs. 4, 5, and 6, where they are compared with the explicit results obtained in the next section.

B. Absolute stability

Without solving the variational problem for the energy stability boundary in the parameter space, we may derive explicit bounds on its location by analyzing the quadratic form directly using various inequalities described in detail in the Appendix. First we note that any divergence-free vector field $\mathbf{u}$ that vanishes at $y = \pm d$ satisfies Poincaré's inequality

$$\langle|\nabla\mathbf{u}|^2\rangle \geq s\left(\frac{\pi}{2d}\right)^2\langle u^2\rangle, \tag{40}$$

where $s = 3.757\ldots$ for divergence-free fields and $s = 1$ without this constraint. The quadratic functional $\mathcal{F}_l[\mathbf{u},\mathbf{b}]$ can be further restricted by using
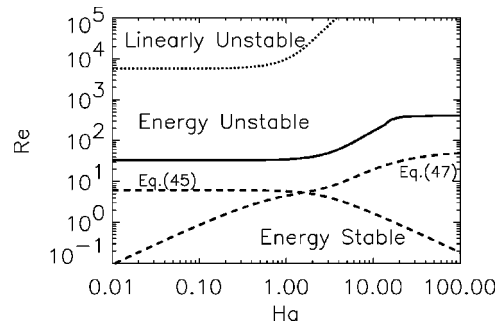

FIG. 6. Critical Reynolds number for Hartmann flow as a function of Ha for $P_m = 0.05$. The solid line is the numerical solution of (39), and the dashed lines are the derived bounds of (45) and (47). The bounds of Sec. III B imply that the laminar solution is energy stable for points below either of the dashed curves. The dotted curve indicates the linear stability threshold obtained by numerical solution.

$$\langle f\mathbf{u}\cdot\mathbf{b}\rangle \leqslant \sup(|f|)\left\langle \frac{u^2}{2c}+\frac{cb^2}{2}\right\rangle, \tag{41}$$

where c is an arbitrary positive number. Inequality (41) is valid for arbitrary fields $\mathbf{u}$, $\mathbf{b}$ and any function f. Applying the Poincaré inequality (40) to the dissipation terms of (33) and inequality (41) to the sign indeterminant terms gives

$$\mathcal{F}_l \geqslant \left[\nu s\left(\frac{\pi}{2d}\right)^2 - \frac{1}{2}\sup(|U_l'|) - \frac{c}{2}\sup(|B_l'|)\right]\langle u^2\rangle$$
$$+ \left[\eta s\left(\frac{\pi}{2d}\right)^2 - \frac{1}{2}\sup(|U_l'|) - \frac{1}{2c}\sup(|B_l'|)\right]\langle b^2\rangle. \tag{42}$$

The quadratic functional $\mathcal{F}_l$ is guaranteed to be strongly positive if each term in the square brackets is positive. Upon adjusting the undetermined number c, we can show that the flow is stable if

$$\left[\frac{1}{2}\sup(|B_l'|)\right]^2 \leqslant \left[\nu s\left(\frac{\pi}{2d}\right)^2 - \frac{1}{2}\sup(|U_l'|)\right]$$
$$\times\left[\eta s\left(\frac{\pi}{2d}\right)^2 - \frac{1}{2}\sup(|U_l'|)\right], \tag{43}$$

where each of the terms in square brackets has to be independently positive.

Applying the above result to Couette flow we obtain the following condition for energy stability:

$$\mathrm{Ha}^2\, R_m^2 \leqslant [s\,\pi^2 - \mathrm{Re}\,\mathrm{Ha}\,\coth(\mathrm{Ha})]$$
$$\times [s\,\pi^2 - R_m\,\mathrm{Ha}\,\coth(\mathrm{Ha})]. \tag{44}$$

Likewise, Hartmann flow is seen to be energy stable if

$$G_m^2[\mathrm{Ha}\,\coth(\mathrm{Ha})-1]^2 \leqslant \mathrm{Ha}^2[s\,\pi^2/2 - \mathrm{Gr}][s\,\pi^2/2 - G_m]. \tag{45}$$

Although inequalities (44) and (45) guarantee (absolute) energy stability, the regions in parameter space that they imply have the unphysical property that for large Hartmann number the Reynolds number must decrease like $\mathrm{Re}\sim 1/\mathrm{Ha}$. The reason for this behavior is that our analysis did not take in to account the boundary layers that would occur in any physical realization. A complementary bound on the location of the curve of marginal stability can be derived by focusing on the behavior of $\mathbf{u}$ and $\mathbf{b}$ near the boundaries. This analysis is carried out in the Appendix, where it is shown that $\mathcal{F}_l$ is positive definite for Couette flow if

$$2R_m^2\left[\frac{1}{\mathrm{Ha}}-\frac{1}{\sinh(\mathrm{Ha})}\right]^2 \leqslant \left[4\sqrt{2}-R_m\frac{\tanh(\mathrm{Ha}/2)}{\mathrm{Ha}}\right]$$
$$\times\left[4\sqrt{2}-\mathrm{Re}\,\frac{\tanh(\mathrm{Ha}/2)}{\mathrm{Ha}}\right] \tag{46}$$

and for Hartmann flow if

$$\frac{1}{2}G_m^2\left[\frac{\mathrm{Ha}+2\tanh(\mathrm{Ha}/2)}{\mathrm{Ha}^2}\right]^2$$
$$\leqslant \left[2\sqrt{2}-\frac{G_m}{\mathrm{Ha}}\left(\frac{1}{\mathrm{Ha}}-\frac{1}{\sinh(\mathrm{Ha})}\right)\right]$$
$$\times\left[2\sqrt{2}-\frac{\mathrm{Gr}}{\mathrm{Ha}}\left(\frac{1}{\mathrm{Ha}}-\frac{1}{\sinh(\mathrm{Ha})}\right)\right]. \tag{47}$$

Figure 4 shows the critical Reynolds number for Couette flow as a function of Ha for $P_m=1$. The solid line is the numerically obtained result, which is compared with the two derived bounds of (44) and (46) (dashed lines). Figure 5 shows the asymptotic behavior of the energy stability boundary for large Hartmann number, which is compared with the bound of (46). The asymptotic value for large P_m is $R_m/\mathrm{Ha}=24$ and for small P_m is $\mathrm{Re}/\mathrm{Ha}=39$. These results differ from those of Ref. 11, which used insulating boundary conditions as opposed to our line-tied conditions. Finally, Fig. 6 shows the critical Reynolds number for Hartmann flow (14) as a function of Ha for $P_m=0.05$. We note that unlike Couette flow, the critical Reynolds number is proportional to Ha only in the range $1\ll\mathrm{Ha}\ll P_m^{-1}$. The reason is that Hartmann flow has magnetic shear in the bulk of the fluid (not at the boundary layers) that can give rise to tearing instabilities (see, for example, Ref. 20 and references therein). In liquid metal experiments this can only be observed for Hartmann numbers of the order $\mathrm{Ha}\sim 10^6$. For both flows the derived bounds seem to capture the dependence of the stability boundary up to a prefactor of order less than 10.

Energy stability is sufficient but not necessary for linear or absolute stability, while linear stability is necessary but not sufficient for absolute or energy stability. Thus, as depicted in Fig. 6 (dotted line), we expect the threshold for linear stability to lie above that for energy stability. This linear threshold was obtained by numerically solving the eigenvalue problem with the line-tied boundary conditions.

IV. BOUNDS ON THE ENERGY DISSIPATION RATE

Next we turn to the derivation of bounds on the energy dissipation rate ϕ or equivalently ψ. We use the decompositions of (24) and (25) of Sec. II C, but this time the background fields $U_b(y)$ and $B_b(y)$ are initially unspecified, to be chosen later to our advantage.

Using (9), (24), and (25) we write the space averaged energy dissipation rate as

$$\mathcal{D}=\nu\left\langle |\nabla\mathbf{u}|^2 + 2U_b'\frac{\partial u_x}{\partial y} + U_b'^2\right\rangle$$
$$+ \eta\left\langle |\nabla\mathbf{b}|^2 + 2B_b'\frac{\partial b_x}{\partial y} + B_b'^2\right\rangle. \tag{48}$$

Dividing (48) by two and adding it to (29) gives

$$\frac{d\mathcal{E}}{dt} + \frac{\mathcal{D}}{2} = \langle u_x B_0 B_b' \rangle + \langle b_x B_0 U_b' \rangle + \langle (b_x b_y - u_x u_y) U_b' \rangle$$

$$+ \langle (u_x b_y - u_y b_x) B_b' \rangle - \frac{\nu}{2} \langle |\nabla \mathbf{u}|^2 \rangle - \frac{\eta}{2} \langle |\nabla \mathbf{b}|^2 \rangle$$

$$+ \frac{\nu}{2} \langle U_b'^2 \rangle + \frac{\eta}{2} \langle B_b'^2 \rangle + \langle F u_x \rangle. \tag{49}$$

In (49) the first two terms are linear in the perturbed quantities, which is undesirable for our subsequent procedure. Thus we remove them with the transformations

$$\mathbf{u} = \mathbf{w} - \mathbf{i} V_b(y), \quad \mathbf{b} = \mathbf{h} - \mathbf{i} H_b(y), \tag{50}$$

where V_b and H_b satisfy

$$\nu V_b'' = B_0 B_b' \quad \text{and} \quad \eta H_b'' = B_0 U_b', \tag{51}$$

with the condition that they vanish at the boundary. Inserting (50) into (49) results in

$$\frac{d\mathcal{E}}{dt} + \frac{\mathcal{D}}{2} = + \langle (h_x h_y - w_x w_y) U_b' \rangle + \langle (w_x h_y - h_x w_y) B_b' \rangle$$

$$- \frac{\nu}{2} \langle |\nabla \mathbf{w}|^2 \rangle - \frac{\eta}{2} \langle |\nabla \mathbf{h}|^2 \rangle + \frac{\nu}{2} \langle U_b'^2 + V_b'^2 \rangle$$

$$+ \frac{\eta}{2} \langle B_b'^2 + H_b'^2 \rangle + \langle F u_x \rangle. \tag{52}$$

Upon time averaging (52), the term $d\mathcal{E}/dt$ vanishes and we are left with an expression for the time averaged rate of dissipation, $\bar{\mathcal{D}}$.

For Couette flow, where $F = 0$, we obtain

$$\bar{\mathcal{D}}_C = \mathcal{D}_b - \bar{\mathcal{Q}}_b, \tag{53}$$

where

$$\mathcal{Q}_b := \nu \langle |\nabla \mathbf{w}|^2 \rangle + \eta \langle |\nabla \mathbf{h}|^2 \rangle - 2 \langle (h_x h_y - w_x w_y) U_b'$$

$$+ (w_x h_y - h_x w_y) B_b' \rangle \tag{54}$$

is a quadratic functional of $\mathbf{w}$ and $\mathbf{h}$ that depends on U_b and B_b, and

$$\mathcal{D}_b := \nu \langle U_b'^2 + V_b'^2 \rangle + \eta \langle B_b'^2 + H_b'^2 \rangle \tag{55}$$

is a functional only of the background fields. For Hartmann flow (52) can be written as

$$\bar{\mathcal{D}}_H = 2F \langle U_b \rangle - \mathcal{D}_b + \bar{\mathcal{Q}}_b, \tag{56}$$

where we used the identity $\langle \mathbf{v} \rangle = \langle \mathbf{i} U_b \rangle + \langle \mathbf{i} u_x \rangle$.

The remaining analysis rests on the fact that if we find two background fields U_b, B_b such that $\mathcal{Q}_b$ is positive definite, then the following inequalities hold for the two flows:

$$\bar{\mathcal{D}}_C \leq \mathcal{D}_b \tag{57}$$

and

$$\bar{\mathcal{D}}_H \geq 2F \langle U_b \rangle - \mathcal{D}_b. \tag{58}$$
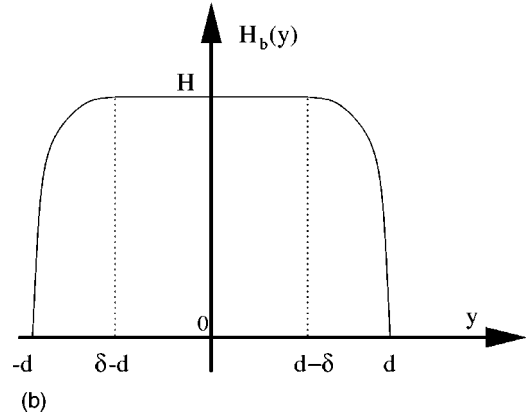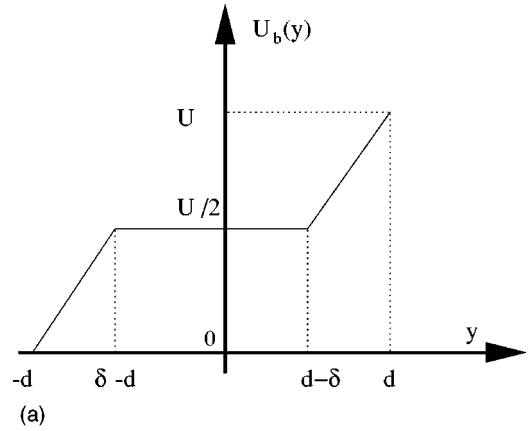

FIG. 7. Panel (a) shows the background field $U_b(y)$ and panel (b) shows $H_b(y)$, where $H := B_0 \delta / 4\eta$.

In the next two sections we identify background fields that make $\mathcal{Q}_b[\mathbf{w}, \mathbf{h}]$ a strongly positive functional and thus determine the bounds on the time average energy dissipation rates of the two flows.

A. Bounds on the dissipation rate of the magnetic Couette flow

The form of $\mathcal{Q}_b$ suggests $B_b \equiv 0$ as the natural choice for the background magnetic field. This choice gives the smallest possible background dissipation and decreases the absolute size of the sign indeterminant term of $\mathcal{Q}_b$. For U_b we choose the piecewise linear profile

$$U_b(y) = \begin{cases} (U/2\delta)(d+y) & \text{if } -d \leq y \leq -d+\delta, \\ U/2 & \text{if } -d+\delta \leq y \leq d-\delta, \\ (U/2\delta)(d-y) & \text{if } d-\delta \leq y \leq d, \end{cases} \tag{59}$$

which is shown in Fig. 7(a). Here δ is a free parameter that will be determined later.

From (51) and the boundary conditions we see that $V_b \equiv 0$ and

$$H_b(y) = \frac{B_0}{\eta} \int_0^y [U_b(y') - \langle U_b \rangle] dy', \tag{60}$$

which is shown in Fig. 7(b).

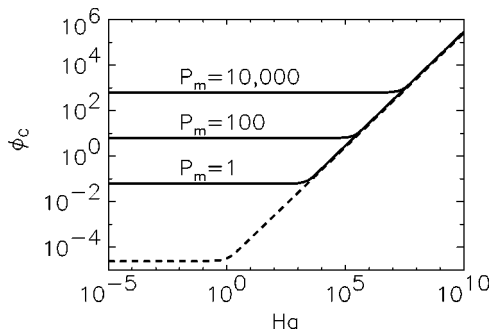With the above choices, the dissipation of the background fields, $\mathcal{D}_b$, is found to be

FIG. 8. Upper bound on dissipation rate for Couette flow as a function of Ha for different Prandtl numbers. The dashed line shows the dissipation of the laminar solution. The Reynolds number Re=10 000 for all cases.
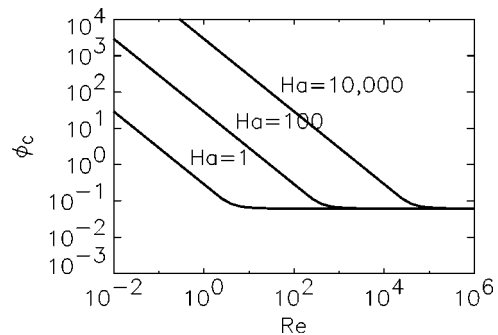

FIG. 9. Upper bound on dissipation rate for Couette flow as a function of Re for different values of Ha. The Prandtl number $P_m=1$ for all cases.

$$\mathcal{D}_b = \frac{\nu U^2}{4d}\left(\frac{1}{\delta} + \frac{B_0^2 \delta}{3\nu\eta}\right). \tag{61}$$

Note, $\mathcal{D}_b$ obtains its minimum value for $\delta_{\min} = \sqrt{3\,\eta\nu/B_0^2}$, giving $\min\{\mathcal{D}_b\} = UB_0/(3\sqrt{3}d)$.

Now we focus on the quadratic term $\mathcal{Q}_b$ and try to determine the values of the free parameter δ that make it positive definite. Formally, we wish to minimize $\mathcal{Q}_b$, and this leads to an eigenvalue problem similar to that of our stability analysis of Sec. III, which we would have to solve numerically. Instead of following this procedure, here we obtain estimates for the values of δ that guarantee the positivity of $\mathcal{Q}_b$, similar to the ones derived in Sec. III B. Using the fundamental theorem of calculus and the Cauchy–Schwartz inequality it is shown in the Appendix that $\mathcal{Q}_b$ is positive definite if

$$\min\{\nu,\eta\} - \frac{U\delta}{4} \geqslant 0. \tag{62}$$

Therefore, $\mathcal{Q}_b[\mathbf{w},\mathbf{h}] \geqslant 0$ if we choose $\delta \leqslant 4\min\{\nu,\eta\}/U = 4d/\max\{\mathrm{Re},R_m\}$. This is the maximum value of δ that our estimates allow, i.e.,

$$\delta \leqslant \frac{4\min\{\eta,\nu\}}{U} =: \delta_Q. \tag{63}$$

The smallest value of $\mathcal{D}_b$ consistent with $\mathcal{Q}_b$ being positive is obtained for $\delta = \min\{\delta_{\min},\delta_Q,d\}$. So we end up with our final result for the Couette flow that if $\delta_{\min} < \delta_Q$ we use $\delta_{\min}$ to evaluate the background dissipation. Therefore,

$$\text{if } \frac{4\min\{\nu,\eta\}B_0}{U\sqrt{3\nu\eta}} > 1, \quad \text{then } \bar{\mathcal{D}}_C \leqslant \frac{U^2 B_0}{2\sqrt{3}d}\sqrt{\frac{\nu}{\eta}}, \tag{64}$$

or in dimensionless form

$$\text{if } 4\,\mathrm{Ha} > \sqrt{3}\max\{\mathrm{Re},R_m\}, \quad \text{then } \phi_C \leqslant \frac{\mathrm{Ha}}{2\sqrt{3}\,\mathrm{Re}}. \tag{65}$$

On the other hand, if $\delta_{\min} > \delta_Q$ we are forced to use δ_Q in the evaluation of the background dissipation. Therefore

$$\text{if } \frac{4\min\{\nu,\eta\}B_0}{U\sqrt{3\nu\eta}} < 1,$$

$$\text{then } \bar{\mathcal{D}}_C \leqslant \frac{\nu}{\min\{\nu,\eta\}}\frac{U^3}{16d} + \frac{\min\{\nu,\eta\}}{\eta}\frac{B_0^2 U}{3d} \tag{66}$$

or in dimensionless form

$$\text{if } 4\,\mathrm{Ha} < \sqrt{3}\max\{\mathrm{Re},R_m\},$$

$$\text{then } \phi_C \leqslant \frac{1}{16}\max\{P_m,1\} + \frac{1}{3}\frac{\mathrm{Ha}^2}{\mathrm{Re}\max\{R_m,\mathrm{Re}\}}, \tag{67}$$

where $\sqrt{3} < \mathrm{Ha}$ and $4 < \max\{\mathrm{Re},R_m\}$ is assumed in the above inequalities so that $\delta < d$ is guaranteed.

In the first inequality (65) we have shown that for large enough magnetic field the dissipation is bounded by a function with the same dependence on Re and Ha as that of the laminar case. The prefactor has only a 15% difference. This gives an indication that the flow should be close to the laminar solution which can be verified at least in the large Ha limit from (45). This behavior is exhibited in Figs. 8 and 9.

On the other hand, if the magnetic field is not strong enough (Ha≪Re), then as shown in Fig. 8 for small Ha and in Fig. 10 for large Re, the dissipation becomes independent of the Reynolds number Re and depends only on the Prandtl number P_m. This agrees with the bound found in Ref. 20 for flows aligned with the magnetic field. Note that we have the same behavior even if the initial magnetic field is zero. That the bound increases with increasing Prandtl number is an
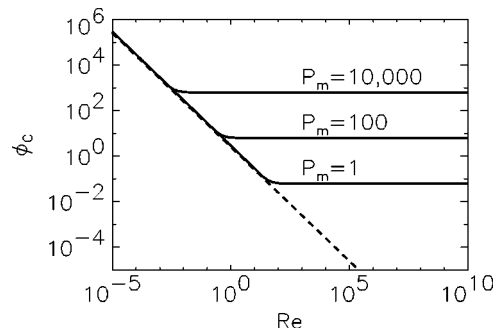

FIG. 10. Upper bound on dissipation rate for Couette flow as a function of Re for different Prandtl numbers. The dashed line depicts the dissipation rate for the laminar solution. The Hartmann number Ha=10 for all cases.
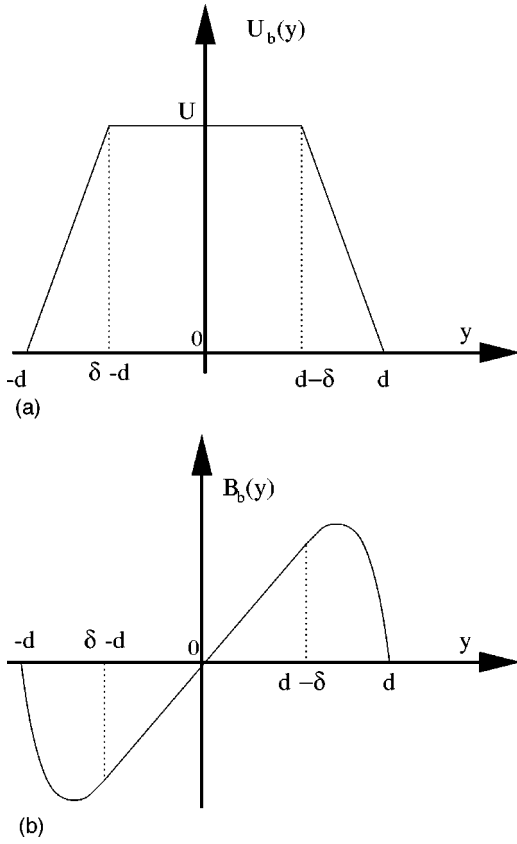
FIG. 11. Panel (a) shows the background field $U_b(y)$ and panel (b) shows $H_b(y)$.

interesting result, yet at present we do not know if it is due to the fact that our estimates are not sharp or if there exists a physical mechanism for the increase of the dissipation.

B. Bounds on the dissipation of Hartmann flow

The procedure for Hartmann flow is similar. Again we make the natural choice for the background magnetic field $B_b \equiv 0$. For U_b we use the piecewise linear profile

$$U_b(y) = \begin{cases} (U/\delta)(d+y) & \text{if } -d \leq y \leq -d+\delta, \\ U & \text{if } -d+\delta \leq y \leq d-\delta, \\ (U/\delta)(d-y) & \text{if } d-\delta \leq y \leq d, \end{cases} \quad (68)$$

where U and δ are free parameters. The background fields $U_b(y)$ and $H_b(y)$ are shown in Figs. 11(a) and 11(b), respectively. Evaluating the background dissipation and $F\langle U_b \rangle$ we get

$$2F\langle U_b \rangle - \mathcal{D}_b = 2FU - FU\left(\frac{\delta}{d}\right) - \frac{\nu U^2}{d^2}\left(\frac{d}{\delta}\right)$$
$$- \frac{B_0^2 U^2}{2\eta}\left[\frac{2}{3}\left(\frac{\delta}{2d}\right) - \left(\frac{\delta}{2d}\right)^2\right]$$
$$\simeq 2FU - \frac{\nu U^2}{d^2}\left(\frac{d}{\delta}\right) - \frac{B_0^2 U^2}{3\eta}\left(\frac{\delta}{d}\right). \quad (69)$$

For convenience, we have dropped the terms $FU\delta/d$ and $B_0^2 U^2 \delta^2/8\eta d^2$, which lead to additional small terms in the

bounds below [viz. $-39\,\mathrm{Gr}^{1/2}/(32\,\mathrm{Ha}^2)$ in Eq. (71) and $-2[1-\mathrm{Ha}^2/(4\max\{\mathrm{Gr},G_m\})]/\max\{\mathrm{Gr}^{1/2},G_m^{1/2}\}$ in Eq. (73)]. The last expression of (69) takes its maximum value when $\delta = \delta_{\min} := \sqrt{3\nu\eta}/B_0$ and $U = U_{\min} := (\sqrt{3}/2)(Fd/B_0)\sqrt{\eta/\nu}$.

Now we turn to the quadratic term $\mathcal{Q}_b$ and try to determine the constraints on δ and U. The calculation is identical to that for Couette flow and gives $\mathcal{Q}_b \geq 0$ if $U\delta \leq 2\min\{\nu,\eta\} = (U\delta)_Q$. Thus, we need only find the values of U and δ that give the maximum possible value of $2F\langle U_b \rangle - \mathcal{D}_b$ without violating the constraint $\mathcal{Q}_b \geq 0$. If $U_{\min}\delta_{\min} \leq (U\delta)_Q$, then the obvious choices for U and δ are $U_{\min}$ and $\delta_{\min}$, respectively. Therefore,

if $U_{\min}\delta_{\min} = \dfrac{3Fd\eta}{2B_0^2} \leq 2\min\{\nu,\eta\}$,

then $\bar{\mathcal{D}}_H \geq \dfrac{\sqrt{3}F^2 d}{2B_0}\sqrt{\dfrac{\eta}{\nu}}$, (70)

or in dimensionless form

if $3\max\{\mathrm{Gr},G_m\} \leq 4\,\mathrm{Ha}^2$, then $\psi_H \geq \dfrac{\sqrt{3}}{2}\dfrac{\mathrm{Gr}^{1/2}}{\mathrm{Ha}}$, (71)

where $\sqrt{3} < \mathrm{Ha}$ is assumed again so that $\delta < d$. If the condition $U_{\min}\delta_{\min} \leq (U\delta)_Q$ is violated then we have to maximize $2F\langle U_b \rangle - \mathcal{D}_b$ over U and δ, with the constraint $U\delta = (U\delta)_Q$. After some algebra we obtain

if $\dfrac{3F\eta}{4B_0^2} \geq \min\{\nu,\eta\}$,

then $\bar{\mathcal{D}}_H \geq \dfrac{8\sqrt{d}}{3\sqrt{3}}\left(F - \dfrac{B_0^2\min\{\nu,\eta\}}{3\eta}\right)^{3/2}\sqrt{\dfrac{\min\{\nu,\eta\}}{\nu}}$ (72)

or in dimensionless form

if $3\max\{\mathrm{Gr},G_m\} \geq 4\,\mathrm{Ha}^2$,

then $\psi_H \geq \dfrac{8}{3\sqrt{3}}\left(1 - \dfrac{\mathrm{Ha}^2}{3\max\{\mathrm{Gr},G_m\}}\right)^{3/2}\min\{1,P_m^{-1/2}\}$, (73)

where the extra condition $6/7 < \max\{\mathrm{Gr},G_m\}$ is assumed so that $\delta < d$.

As in the Couette case, for strong enough magnetic field the first inequality (71) indicates that the bound is very close (within 15%) of the laminar dissipation rate. On the other hand, for small enough magnetic fields the bound on the dissipation becomes independent of Ha and Gr, and decreases as the inverse square root of the Prandtl number for $P_m > 1$. This result is not in contradiction with the related result for Couette flow which has a linear increase with the Prandtl number. The reason for the difference lies in the definition of the dimensionless dissipation. If we use ϕ_H instead of ψ_H, as given by Eq. (16), the lower bound becomes an upper bound and we obtain the same scaling with the Prandtl number. Figures 12, 13, and 14 summarize these results for Hartmann flow.
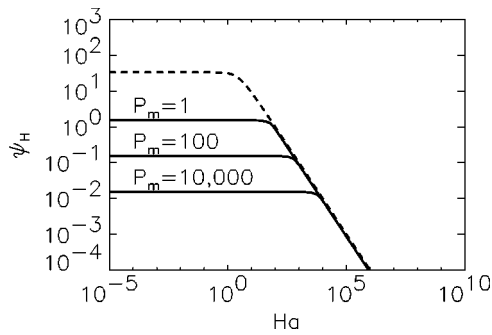
FIG. 12. Lower bound on the dissipation rate for Hartmann flow as a function of Ha for different Prandtl numbers. The dashed line shows the dissipation rate of the laminar solution. The Grashoff number Gr= 10 000 for all cases.

FIG. 14. Lower bound on the dissipation rate for Hartmann flow as a function of Gr for different values of Ha with $P_m = 1$ for all cases.

V. DISCUSSION

We have studied the energy stability boundary and properties of the dissipation rate for two MHD flows with an imposed cross-stream magnetic field, magnetic Couette flow and Hartmann flow. The flows were determined to be energy stable in the regions in the parameter space determined by inequalities (44), (45), (46), and (47). The energy stability equations were solved numerically and the same qualitative behavior, up to a numerical prefactor, as that of the analytic results was obtained. We derived bounds on the dissipation rates and determined their behavior at high Reynolds and magnetic Reynolds numbers. One of our basic results is that the dissipation tends to the laminar value if the magnetic field is strong enough. If the magnetic field is not very strong and the Reynolds number is large, then the bound is independent of Re and Ha and scales as the first power of the Prandtl number if $P_m > 1$. Otherwise, the bound is independent of the Prandtl number.

Figure 15 shows a quantitative comparison of experimental data from Ref. 5 with our bound. The data show measurements of the drag coefficient C_f that is equal to ϕ_H as a function of Ha/Re. Although there is a two orders of magnitude discrepency with our bound, which is not surprising because of the rough estimates used, the bound appears to capture the behavior of the dissipation up to a prefactor.
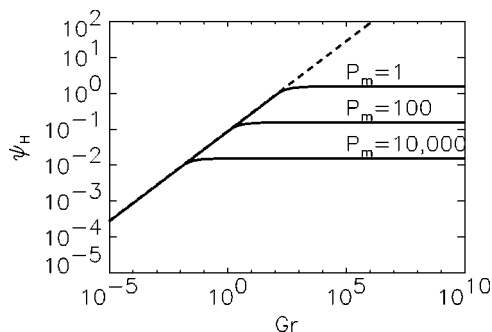
Finally we note that a number of unresolved issues remain. First, better estimates of the bounds in Sec. IV can be made by solving directly the eigenvalue problem. Furthermore, only energy constraints were used to restrict the dissipation rate, and it would be interesting to investigate the possibility that the helicity and cross-helicity constraints might improve our results. Last, the relevance of the dependence of the bound in (67) and (73) with the Prandtl number should be further investigated, either in experiments or numerical simulations.

ACKNOWLEDGMENTS

APPENDIX: PROOFS OF EQS. (46), (47), AND (62)

For any function $f(x,y,z)$ that satisfies $f(x,-d,z)=0$, we have from fundamental theorem of calculus

$$f(x,y,z) = \int_{-d}^{y} \frac{\partial f(x,y',z)}{\partial y'} dy'. \qquad \text{(A1)}$$

FIG. 13. Lower bound on the dissipation rate for Hartmann flow as a function of Gr for different Prandtl numbers. The dashed line shows the dissipation rate of the laminar solution. The Hartmann number Ha=10 for all cases.
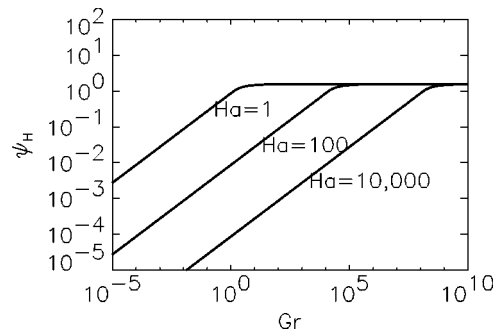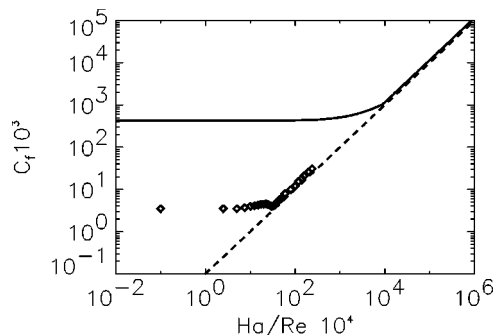

FIG. 15. Drag coefficient C_f as a function of Ha/Re. The diamonds are experimental data from Ref. 5 for Re=5×10^5. The dashed line is the drag coefficient for the laminar solution and the solid line is the upper bound.

Using the Schwartz inequality we can show that

$$|f| \leq \sqrt{y+d} \left(\int_{-d}^{0} \left| \frac{\partial f(x,y',z)}{\partial y'} \right|^2 dy' \right)^{1/2} \tag{A2}$$

and similarly for the upper boundary $(+d)$. Using the inequality $|ab| \leq a^2/(2c) + cb^2/2$ for any $c>0$ and combining the upper with the lower part of the domain we can prove the following inequality for a piece of the functional of (33):

$$\langle U_l' u_x u_y \rangle \leq \left\langle \frac{1}{c} \left(\frac{\partial u_x}{\partial y} \right)^2 + c \left(\frac{\partial u_y}{\partial y} \right)^2 \right\rangle \frac{1}{2} \int_{-d}^{0} |U_l'|(d+y)dy, \tag{A3}$$

where we have used the fact that $|U_l'|$ is a symmetric function. A similar result follows for B_l' and all the combinations of the fields u_x, u_y, b_x, and b_y. The divergence-free condition, some integration by parts, and application of the Schwartz inequality imply

$$\left\langle \left(\frac{\partial u_y}{\partial y} \right)^2 \right\rangle \leq \left\langle \left(\frac{\partial u_x}{\partial x} \right)^2 + \left(\frac{\partial u_x}{\partial z} \right)^2 + \left(\frac{\partial u_z}{\partial x} \right)^2 + \left(\frac{\partial u_z}{\partial z} \right)^2 \right\rangle. \tag{A4}$$

Using $c=1/\sqrt{2}$ for the $\langle (u_x u_y - b_x b_y) U_l' \rangle$ term, we can show the following inequality for the functional $\mathcal{F}_l$ of (33):

$$\mathcal{F}_l \geq \left[\nu - \frac{1}{2\sqrt{2}} \int_{0}^{+d/2} |U_l'| \left(\frac{d}{2} - y \right) dy \right.$$

$$\left. - \frac{1}{2c} \int_{0}^{+d/2} |B_l'| \left(\frac{d}{2} - y \right) dy \right] \langle |\nabla \mathbf{u}|^2 \rangle$$

$$+ \left[\eta - \frac{1}{2\sqrt{2}} \int_{0}^{+d/2} |U_l'| \left(\frac{d}{2} - y \right) dy \right.$$

$$\left. - \frac{c}{2} \int_{0}^{+d/2} |B_l'| \left(\frac{d}{2} - y \right) dy \right] \langle |\nabla \mathbf{b}|^2 \rangle. \tag{A5}$$

This functional is positive definite if each term in the square brakets is positive. Eliminating c from the resulting inequalities and performing the integrations leads to (46) and (47). An identical calculation using U_b and B_b instead of the laminar solutions for the functional $\mathcal{Q}_b$ leads to the result in (62).

[1] J. Hartmann, Mat. Fys. Medd. K. Dan. Vidensk. Selsk. **15**, No. 6 (1937).
[2] J. Hartmann and F. Lazarus, Mat. Fys. Medd. K. Dan. Vidensk. Selsk. **15**, No. 7 (1937).
[3] C. B. Reed and P. Lykoudis, J. Fluid Mech. **89**, 147 (1978).
[4] P. Lykoudis, Rev. Mod. Phys. **32**, 796 (1960).
[5] R. A. Gardner and P. Lykoudis, J. Fluid Mech. **47**, 737 (1971).
[6] G. Branover, Magnetohydrodynamics (N.Y.) **3**, 3 (1967).
[7] S. Lundquist, Ark. Fys. **5**, 297 (1952).
[8] R. C. Lock, Proc. R. Soc. London, Ser. A **223**, 105 (1955).
[9] M. Takashima, Fluid Dyn. Res. **17**, 293 (1996).
[10] M. Takashima, Fluid Dyn. Res. **22**, 105 (1998).
[11] R. J. Lingwood and T. Alboussiere, Phys. Fluids **11**, 2058 (1999).
[12] L. N. Howard, J. Fluid Mech. **17**, 405 (1963).
[13] L. N. Howard, Annu. Rev. Fluid Mech. **4**, 473 (1972).
[14] F. Busse, Adv. Appl. Mech. **18**, 77 (1972).
[15] C.-B. Kim and J. Krommes, Phys. Rev. A **42**, 7487 (1990).
[16] C. Y. Wang, A. Bhattacharjee, and E. Hameiri, Phys. Fluids B **3**, 715 (1991).
[17] C. Y. Wang and A. Bhattacharjee, Phys. Fluids B **3**, 3462 (1991).
[18] C. R. Doering and P. Constantin, Phys. Rev. E **49**, 4087 (1994).
[19] C. R. Doering, E. A. Spiegel, and R. A. Worthing, Phys. Fluids **12**, 1955 (2000).
[20] F. Pétrélis, A. Alexakis, C. R. Doering, and P. J. Morrison, Phys. Plasmas **10**, 4314 (2003).
[21] R. R. Kerswell, Physica D **121**, 175 (1998).